EBioMedicine 62 (2020) 103119

Contents lists available at ScienceDirect

EBioMedicine

journal homepage: www.elsevier.com/locate/ebiom

Research paper

Evidence for liver and peripheral immune cells secreting tumor-suppressive extracellular vesicles in melanoma patients

Jung-Hyun Lee[1,a], Martin Eberhardt[a], Katja Blume[a], Julio Vera[a], Andreas S. Baur[*,a]

[a] Department of Dermatology, University Hospital Erlangen, Hartmannstr. 14, 91054 Erlangen, Germany

ARTICLE INFO

Article History:
Received 10 January 2020
Revised 23 October 2020
Accepted 26 October 2020
Available online xxx

Keywords:
Plasma extracellular vesicles (pev)
Pev origin
Liver cells
Circulating tumor cells
miRNA
Pro-inflammatory cytokines
Melanoma.

ABSTRACT

Background: Before and after surgery melanoma patients harbor elevated levels of extracellular vesicles in plasma (pEV), suppressing tumor cell activity. However, due to technical reasons and lack of cell-specific biomarkers, their cellular origin remains obscure.
Methods: We mimicked the interaction of tumor cells with liver cells and PBMC in vitro, and compared newly secreted EV-associated miRNAs and protein factors with those detected in melanoma patient`s pEV.
Findings: Our results suggest that pEV from melanoma patients are secreted in part by residual or relapsing tumor cells, but also by liver and peripheral blood mononuclear cells (PBMC). Our approach identified factors that were seemingly associated either with tumor cell activity, or the counteracting immune system, including liver cells. Notably, the presence/absence of these factors correlated with the clinical stage and tumor relapse.
Interpretation: Our study may provide new insights into the innate immune defense against tumor cells and implies that residual tumor cells could be more active than previously thought. In addition we provide some preliminary evidence that pEV marker patterns could be used to predict cancer relapse.

1. Research in context

1.1. Evidence before this study

Plasma extracellular vesicles (pEV) circulate in high concentrations through the bloodstream, but their cellular origins remain obscure due to technical reasons and lack of tissue-specific biomarkers. While miRNA and mutational signatures in pEV have been used to analyze pEV in bulk preparations, these markers are not suitable to differentiate pEV subpopulations. Hence little is known about the quantity and function of pEV subpopulations in cancer patients. However, it would be of great importance to learn about the origin of pEV, and their respective role in the interaction between the immune system and tumor cells.

1.2. Added-value of this study

In view of the described difficulties we used an indirect method in conjunction with bioinformatics and an algorithm, comparing EV biomarker patterns of EV proteins and miRNAs obtained in vitro with those found in pEV of melanoma patients. While this approach could not give definite answers, it provided preliminary evidence that the pEV population changes upon cancer development or relapse, harboring vesicle populations derived from cancer cells, but also from the innate immune system. Furthermore, we demonstrate that these biomarker patterns could be suitable to predict disease progression.

1.3. Implications of all the available evidence

The implications of this study are twofold. First, it appears that the innate immune system, particularly liver cells and PBMC, react to cancer development in part by secreting tumor cell-suppressive pEV. Second, patterns of pEV biomarkers in conjunction with bioinformatics may help to better predict the course of the disease.

2. Introduction

Human plasma is considered to harbor a high concentration and mixture of plasma EV (pEV) of different cellular origin. However, confirmed or accepted numbers for pEV, or specific subpopulations thereof, are lacking. This is due to technical difficulties in identifying and discriminating vesicles. In addition, the great variability of pEV with respect to size, surface marker composition, cellular and subcellular origin further complicates this task. Nevertheless it was suggested that a significant portion of pEV are secreted by platelets,

* Corresponding author.
E-mail address: andreas.baur@uk-erlangen.de (A.S. Baur).
[1] current address.

https://doi.org/10.1016/j.ebiom.2020.103119

namely up to 10^7/ml plasma, as determined by flow cytometry [1]. Notably, these pEV were found to have multiple effects on target cells in homeostasis and disease [2].

There is accumulating evidence suggesting that cancer cell-derived pEV harbor specific biomarkers [3, 4]. However, there is insufficient knowledge on their relative blood concentration in different stages of the disease, particularly after complete (R0) tumor surgery. Complicating the situation, cancer cells may stimulate host cells to secrete additional pEV populations. Tumor cells and their secreted EV may stimulate immune cells and/or the tumor microenvironment, for tumor-suppressive or tumor promoting effects [5, 6]. For example, senescent tumor cells secrete the senescence-associated secretory phenotype (SASP), consisting of a whole array of pro-inflammatory soluble and insoluble factors, able to stimulate fibroblasts of the tumor microenvironment [7]. Notably, EV are part of the SASP and may contributes to a pro-inflammatory remodeling of the tumor microenvironment [8].

After purification by differential centrifugation and sucrose gradient, we determined that healthy individuals harbor around 10^9–10^{10} EV per milliliter plasma. This vesicle concentration increased between 4 and 20fold in disease conditions, like malignant melanoma and HIV infection, and remained at higher levels after primary tumor resection or anti-retroviral therapy [9],[10]. The relative pEV increase was corroborated by measuring vesicle-associated micro-RNA levels and protein concentrations in EV sucrose gradient fractions. However, it remained unclear from which cell population (s) these increased pEV levels was/were secreted.

Since we found that elevated pEV after R0 surgery were tumor-suppressive [9], and since pEV have a rather short life span of about 10–30 min [11, 12], a sizable and active cell population or organ had to be assumed, serving as their cellular source. On the other hand, a tumor cell-derived secretion seemed possible, although the in general low concentration of circulating or disseminated tumor cells (CTC/DTC) [13], as well as their assumed tumor promoting function, suggested a minor contribution to the increased pEV levels after surgery.

In view of the difficulties to determine the cellular origin of pEV, we analyzed the EV content derived from co-cultures of PBMC and liver cells with tumor cells in vitro. We hypothesized that this co-culture mimicked the interaction of these cells in vivo, leading to newly secreted EV with a particular factor pattern. This pattern would not necessarily be specific for tumor cells, but representative for the interaction of these cell populations. We reasoned that similar marker patterns would be detected in patient's pEV, if our assumption was correct. To validate this approach, we assessed two different sets of markers, namely cytokines, chemokines and soluble factors (CCF), and micro-RNAs. In summary, the results supported our hypothesis, implying an increased secretory activity of liver cells and PBMC upon encounter of tumor cells. To our surprise, our data also hinted at a notable secretory activity of residual and relapsing tumor cells. Our study may provide insights into the interaction of tumor cells with the host immune system that potentially could be exploited for diagnostic purposes.

3. Material and methods

Cell lines and primary cells. Liver cell lines Huh7 (RRID: CVCL_0336) and Sk-Hep-1 (RRID: CVCL_0525) (kindly provided by P. Knolle, Technische Universität München) were grown in DMEM (Sigma-Aldrich) supplemented with 10% Fetal calf serum (FCS, Sigma-Aldrich) and 1% penicillin-streptomycin (Lonza). Sk-Hep1 cells were additionally maintained in 40 μM β-mercaptoethanol (Carl Roth). LX-2 (RRID:CVCL_5792) cells were provided by SL. Friedman (Icahn School of Medicine, New York) and cultured in DMEM high glucose (Life Technologies) supplemented with 2% FCS, 1% penicillin-streptomycin. All cells were grown at 37 °C under 5% CO_2. Peripheral blood mononuclear cell (PBMC) preparation: Leukoreduction system chambers (LRSCs) from healthy donors were acquired after plateletpheresis. The resulting platelet free cell sample was diluted 1:2 in PBS and the PBMC containing buffy coat was isolated after density gradient centrifugation on Lymphoprep (Axix Shield 1,114,544). Generation of immature/mature Dendritic cells (DC): Monocytes were isolated from PBMCs using BD IMag Anti-Human CD14 Magnetic Particles (BD Biosciences 557,769). 6.0×10^6 monocytes were seeded in a 6 well plate in RPMI supplemented with 1% human serum (Sigma-Aldrich). Monocyte-derived DC were generated adding 800 IU/ml of recombinant GM-CSF and 250 IU/ml of recombinant IL-4 (both from CellGenix). For EV isolation (see below) immature DC were washed and 24 h later the supernatant was harvested (10 ml). To generate mature DC, immature DC cultures were supplemented for 24 h with LPS (100 ng/ml) or a maturation cocktail (200 IU/ml IL-1ß, 1000 IU/ml IL-6 (both from CellGenix), 10 ng/ml TNF (beromun; Boehringer Ingelheim) and 1 μg/ml Prostin E2 (PGE2, Pfizer). Subsequently cells were washed and EV supernatants (10 ml) were collected 24 h later for EV isolation. Generation of Macrophages: Monocytes were separated from the non-adherent fraction (NAF) by plastic adherence on cell culture flasks and cultured in RPMI supplemented with 1% human serum and 1% of penicillin/streptomycin. On days 1, 3, 5, 7 and 9 medium was supplemented with 800 IU/ml of GM-CSF. On day 11, medium was removed, cells were washed and 20 ml of RPMI supplemented with 1% of EV depleted human serum was added. After 24 h the supernatant was harvested and EV were isolated. For all procedures see also [10]. MCTC cell line: From 30 ml blood of a melanoma patient the CD45-positive cells were depleted using CD45 RosetteSep (Stemcell Technologies) according to manufacturer's instructions. The remaining cells were stained with MCSP-APC and MCAM-FITC antibodies (both from Miltenyi) and DAPI (Thermo Fisher) for dead cell exclusion. MCSP-positive and/or MCAM-positive cells were then sorted on a FACS Aria SORP (BD) cell sorter and seeded in RPMI cell culture medium with 20% human pooled serum. Medium was replaced on a regular basis and cells showed first signs of growth after several weeks. At the time the CTC cells were obtained the patient was tumor free. Melanoma lines ML-1IK, ML-2Sc and ML-3So: Melanoma tumor cell lines were generated as described before [14]. Briefly, fresh tumor biopsies were obtained directly after surgery. A single cell suspension was produced by mechanical dissociation and enzymatic digestion with DNAse and collagenase. Cells were seeded in RPMI supplemented with 20% human serum into 6-well plates. Passaging of cells was performed according to cell density. A later analysis revealed that all lines were positive for BRAFV600E. Primary fibroblasts were obtained from Thermo Fisher Scientific (C0135C) and cultured in DMEM with 10% FCS.

3.1. EV depletion of FCS and human serum for cell culture

To assure that EV generated from cell culture were not contaminated by outside sources, heat-inactivated FCS and human serum for medium supplementation were depleted of bovine EV by ultracentrifugation for 18 h at 110,000 g and 4 °C before use.

3.2. Antibodies and reagents

Primary antibodies were used at 1–2 μg ml^{-1} for immunoblotting: anti-ADAM10 (mouse monoclonal, Abcam ab73402), anti-CD63 (mouse monoclonal, BD Biosciences 556,019), anti-CD81 (mouse monoclonal, BD Biosciences 555,675), anti-Haptoglobin (rabbit polyclonal, Biozol, GTX 112,962–25). The following secondary antibodies were used: Alexa Fluor 488 goat anti-mouse and Alexa Fluor 555 goat anti-rabbit IgG (both from Life Technologies) and anti-mouse IgG-HRP conjugate and anti-rabbit IgG-HRP conjugate (both from Cell Signaling).

3.3. Patient material

Cohort 1 (Fig. 1A): This is the same patient cohort described in Lee et al., 2019. Briefly, Plasma samples were obtained from patients attending the outpatients departments at the University Hospital Erlangen after signing an informed consent. The study was approved by the local ethics committee in Erlangen (Nr. 4602). Patients were assigned to the respective study groups based on their clinical stage [15]. R0 operated patients were subdivided into high risk (HR) (stage II-IV) and low risk (LR) patients (stage I). T patients harbored tumor metastases (clinical stage III and IV), or primary tumors (clinical stage I – II) before surgery.

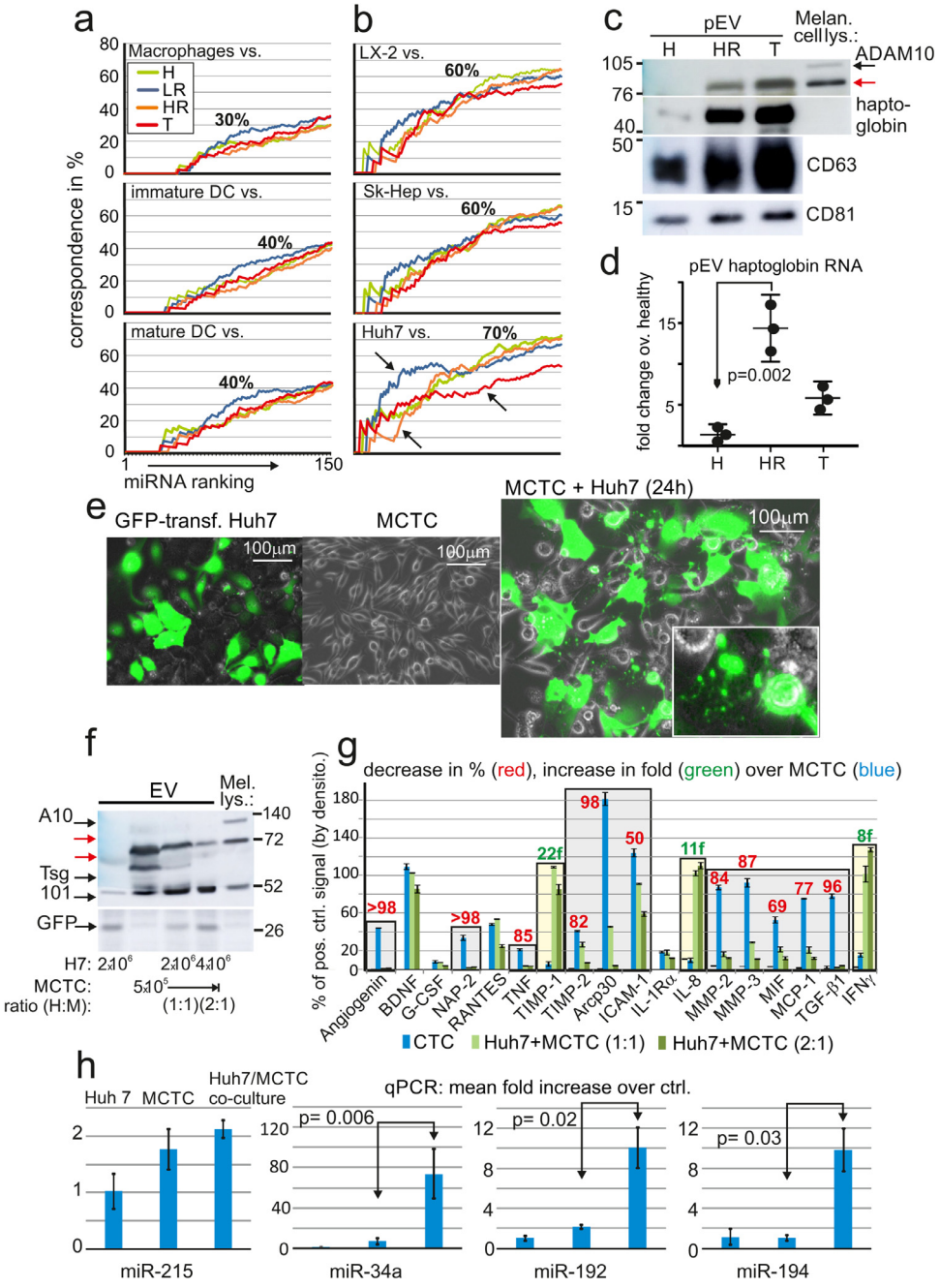

Fig. 1. Hepatocytes are a possible source of melanoma-suppressive pEV a-b Relative similarity of pEV miRNA profiles with cell-derived EV profiles using correspondence at the top (CAT) plots. a Pairwise similarity (correspondence in%) of 150 ranked miRNAs from EVs derived from myeloid cells (mature DC, immature DC, macrophages) and b liver cells (Huh7, SkHep-1, LX-2), which were compared with pEV-derived miRNAs from healthy individuals (H) and melanoma patients (LR-, HR- and T-patients; see text for explanation). Arrows indicate deviation of correspondence from control (Healthy). c Presence of haptoglobin in melanoma pEV. Plasma EV from one healthy individual and one HR and T-patient were gradient purified and blotted for the indicated pEV markers and haptoglobin as indicated. A melanoma cell lysate served as control for ADAM10. d Relative amount of haptoglobin mRNA in melanoma pEV compared to healthy donor pEV. Error bars represent SDM based on analyses of pEV from 3 different donors in each clinical stage. e Images of GFP-transfected Huh7 and melanoma MCTC cells cultured separately or co-cultered over 48 h at a ratio of 1:1. f Assessment of ADAM10 (A10) and Tsg101 (EV marker) by Western blot in EV lysates derived from cultures and co-cultures of Huh7 and CTC cells (90 ml supernatant), cultured in different ratios (1:1; 2:1). *M* = MCTC cells. H7 = Huh7 cells. The overall cell number of MCTC cells remained the same (5×10^5), the number of Huh7 cells increased to 10^6. One lane represents the amount of EV purified from 15 ml supernatant. g Quantification of indicated factors assessed by protein array (primary data in Supplementary Fig. 1b) in EV secreted by cell cultures described in (f) (purified from equal culture volume). Primary data were quantified by densitometry and calculated in% from the positive controls (pos.) on each blot. Co-culture of Huh7 and MCTC cells were done with different cell ratios as indicated. Gray and yellow boxes are described in the text. A decrease of EV-associated factors from levels found in MCTC cultures is indicated by red numbers, an increase by green numbers. Error bars represent SDM based on four values of two experiments (Supplementary Fig. 1b). h Quantitative PCR analysis on indicated miRNAs in EV obtained from cell culture supernatants described in (e). Bar diagrams depict the average fold-increase over an internal control miRNA of the commercial assay. Error bars represent the SDM of triplicate PCR runs, One representative experiment out of three is presented. P-values by two-tailed Students *t*-test.

Cohort 2 (Fig. 2, 4, 5): Plasma samples were obtained as for cohort 1, with the exception of *Re*-patients, and were otherwise categorized in LR and HR patients. In *Re* patients (relapsing patients), the blood sample was taken upon tumor relapse, detected at routine clinical presentations (every 3 month) or upon ad hoc presentations after patients detected a new growing lump. A summary of the patient data is listed in Supplementary Table 2.

3.4. CAT plots (patient cohort 1)

The CAT (correspondence at the top) plots were generated with miRNA data obtained from pEV/EV of patient cohort 1 and primary immune cells (mature and immature dendritic cells, macrophages). The miRNA assessment by a commercial provider was described in [9]. The miRNA extraction is described below. For the CAT plot analysis we adapted a method used previously to compare the agreement in measurements between microarray platforms [16]. Each trace in the graphs (Fig 1a) corresponds to one comparison between two groups, as indicated by the legend. Specifically, the traces show the percentage of common miRNAs in two group rankings plotted against rank. To rank the miRNAs in each group, the mean (m) and standard deviation (SD) of miRNA EV concentrations were estimated as follows: For all groups (or cells) there was only one measurement available (n = 1), so m was set to signal intensity and SD to signal error, as recorded by the instrument. A score S for every microRNA was calculated according to $S = m / SD$, and miRNAs were ranked by sorting S in descending order for each group.

3.5. miRNA assessment and analysis for patient cohort 2

The miRNA content of pEV (see below), was reverse transcribed into cDNA as described previously [9]. Subsequently the miRNA quantification was performed on the NanoString platform according to the manufacturer`s instructions using the respective miRNA assessment and quantification kit (GXA-MIR3−12). Resulting counts were subjected to background correction based on negative controls and global normalization in R (R Core Team (2018). R: A language and environment for statistical computing. R Foundation for Statistical Computing, Vienna, Austria. https://www.R-project.org/) with the package NanoStringQCPro (https://doi.org/doi:10.18129/B9.bioc.NanoStringQCPro). An additional round of quantile normalization was applied separately to the patient samples (n = 20) and the cell population samples (n = 44), respectively. Afterwards, replicate means were calculated for each patient and culture category and separated into three reference groups: patient-derived blood plasma, in vitro monocultures and in vitro co-cultures. In each of these groups independently, miRNAs were analyzed for overrepresentation by checking if the normalized expression value exceeded the highest value from the reference categories (Supplementary Table 3) by at least two-fold. MiRNAs for which this test turned out positive were deemed to be associated with the corresponding category. Using R and the package VennDiagram (https://CRAN.R-project.org/package=VennDiagram), the overlap of associated miRNAs between selected categories was then inspected with Venn diagrams (Fig. 2b).

3.6. Isolation and purification of EV and pEV

EV and pEV purification was performed essentially as described previously [10]. Briefly, cell culture supernatants were collected after 48 h and centrifuged for 20 min at 2000 g, 30 min at 10,000 g and ultra-centrifuged (rotor: TH641 (Thermo Fisher Scientific)) for 1 h at 100,000 g, all at room temperature (4 °C). Pellets were resuspended in 35 ml PBS and centrifuged at 100,000 g for 1 h. Pellets were resuspended in 100 μl PBS and considered as EV preparations. For pEV purification, 10 ml blood plasma was diluted with 10 ml PBS and centrifuged for 30 min at 2000 g, 45 min at 12,000 g and ultra-centrifuged (rotor: TH641) for 2 h at 110,000 g, all at 4 °C. Pellets were resuspended in 10 ml PBS and centrifuged at 110,000 g for 1 h. Pellets were again resuspended in 100 μl PBS and considered as EV preparations. These Pellets were solubilized in SDS sample buffer or re-suspended in 100 μl PBS and aliquots were analyzed by immunoblotting or Cytokine/Chemokine/ soluble Factor (CCF) protein array (see below). For each sample particle concentration and size distribution was determined using particle tracking (ZetaView®) (see Supplementary Fig. 2A)

3.7. Human cytokine/chemokine/soluble factor (CCF) array

Purified EV or pEV corresponding to equal volume of cellular supernatant (in general 60 ml from 10 mio. transfected cells) or equal plasma volume (1 ml) were applied to the RayBio Human Cytokine Array C-S (Hölzel Diagnostika, AAH—CYT-1000−2) according to the manufacturer's instructions. A minimum of 20 μg EV proteins was used per filter incubation. Spot signal intensities were quantified with the ImageJ plugin Protein Array Analyzer. For cross-blot normalization, subtraction of the average intensity of blank spots (n = 14) and division by the average of the positive controls was performed. A list of factors of interest was then selected and plotted in a Euclidean-distance heat map using the library heatmap in R (https://CRAN.R-project.org/package=pheatmap). For a control experiment (Supplementary Fig. 6b) a selected set of CCF factors were quantified using the BioLegend LEGENDplex™ kits: Human proinflammatory Chemokine panel (Cat No. 740,003, lot B 254,807). The absolute concentration of each factor was determined using the LEGENDplex™ data analysis software based on a standard curve recorded for each factor and run. The LEGENDplex assay captures molecules through beads coated with specific antibodies. Specific biotinylated antibodies then bind to the captured molecules and are recognized by dye-coupled streptavidin. The dye signal intensities are quantified in a flow cytometer.

3.8. Quantitative PCR amplification

The procedure was described in detail in [9]. Reverse transcription of extracted pEV RNA was performed using the commercially available QantiTect Reverse Transcription kit (Qiagen, Cat. No: 205,311) or TaqMan® MicroRNA Reverse Transcription Kit (ThermoFisher, Cat. No: 4,366,596) using commercially available TaqMan® MicroRNA Assays (ThermoFisher, Cat. No: Cat. # 4,427,975). For amplification of miRNAs, qRT-PCR was performed using TaqMan® MicroRNA Assays (ThermoFisher, Cat. No: Cat. # 4,427,975) with a Rotor-Gene Probe PCR Kit (Qiagen, Cat. No: # 204,374) according to the manufacturer's instructions on a Qiagen Rotor-Gene Q real time PCR-cycler.

3.9. Particle quantification

Sucrose-purified pEV were diluted 1:1000 in PBS. The pEV numbers were quantified via particle tracking analysis on a commercially available ZetaView® particle tracker from ParticleMetrix (Meerbusch, Germany) using a 10 μl aliquot of the diluted samples. The concentration of pEV was calculated based on the dilution factors.

3.10. Statistics

Patient samples and cell culture samples were analyzed without prior sample size determination, randomization, or blinding. No measurements were excluded from the analysis. Data were statistically evaluated using Student's t-test or One-Way ANOVA subsequently followed by Tukey's honest significant difference test when applicable. The numbers of miRNAs assigned to different culture conditions were compiled in overlap-derived contingency tables (Fig. 2c); then, chi-squared tests for imbalances in the observed frequencies were performed and p-values corrected according to the

method proposed by Benjamini et al. [17] to control the false discovery rate.

3.11. Role of funding source

The public funding sources were providing support for personnel and consumables. They were not involved in the study design, data collection, data analyses, interpretation or writing of the manuscript.

4. Results

4.1. Evidence for Hepatocytes as one possible source of pEV

In post-surgery melanoma patients, we found pEV levels to be significantly increased [9]. Conversely, residual tumor cells (CTC/DTC) are usually identified at very low frequency (10^{-5}–10^{-6}) in bone marrow and lymph nodes [13]. We therefore assumed that a major fraction of elevated melanoma pEV were of non-tumor origin, for example from the innate immune system. To test this assumption, we compared miRNA profiles from EV secreted by primary immune cells, with those of patient`s pEV and healthy controls. For this analysis the same patient data sets were used as described in our recent study [9]. In that study, patients had been subdivided into those with a high risk (HR) and those with a low risk (LR) for tumor relapse, and those bearing a tumor (T).

We employed correspondence at the top (CAT) plots [18], comparing EV/pEV miRNA profiles that were ranked by relative miRNA concentrations, assuming that profiles from the same cell linage have a similar ranking. A pairwise comparison of the 150 highest-ranked miRNAs, revealed that EV-derived miRNA profiles from primary immune cells with secretory activity (macrophages, immature and mature DC) had only a low correspondence with patient`s pEV-derived profiles (30−40%), and no noticeable difference between patients and healthy controls was observed (Fig. 1a). Hence, either a different cell population was the source of elevated melanoma pEV, or our assumption or experimental approach was not correct.

Recently we found evidence that pEV in HIV patients are secreted in part by the liver [19], an organ with a high secretory activity. We therefore included EV miRNA profiles derived from 3 liver cell lines into our analysis, representing parenchymal (Huh7), hepatic stellate (LX-2) and liver sinus endothelial cells (SK-Hep). Using CAT plot analysis, liver miRNA profiles revealed a much higher overall correspondence with patient`s pEV and also healthy controls (60−70%), implying that at least a portion of pEV could have derived from liver cells. (Fig. 1b). Notably, when compared with hepatocyte (Huh7)-derived EV profiles, melanoma patient pEV miRNA profiles differed from healthy controls (Fig. 1b, arrows). This hinted at hepatocytes as at least one possible source of cancer-induced pEV.

As these results were merely an indication for our assumption, we analyzed patient pEV for liver-specific factors. We found that haptoglobin, a liver acute phase protein, was incorporated in significant amounts (Fig. 1c). We could also demonstrate an upregulation of its mRNA in pEV from patients bearing a tumor (T) or having a high risk (HR) for tumor relapse (Fig. 1d). This supported our assumption that hepatocytes could be at least one possible source for melanoma-induced pEV.

4.2. Upon tumor cell co-culture hepatocytes secrete tumor cell suppressive EV

To substantiate our findings, we decided to mimic an assumed interaction of hepatocytes with circulating tumor cells (CTC) in cell culture. We assumed this would induce hepatocyte EV secretion with tumor-suppressive properties, as implicated by the results of our previous study [9]. Besides Huh7 hepatocytes we employed a melanoma CTC cell line (MCTC) established from peripheral blood of a patient in our department (see materials and methods for details).

Upon co-culture (24 h) GFP-transfected Huh7 cells started a noticeable secretory activity, evidenced [1] by the appearance of green vesicular structures (Fig. 1e, panel 3) and [2] by an increase of particle/vesicle concentration in culture supernatants of more than 10fold over EV produced by cells without co-culture (Supplementary Fig. 1a).

To assess the consequences of this effect for the tumor cells, EV were purified from these culture supernatants and analyzed for a marker typically found in melanoma cell-derived EV and pEV, namely ADAM10 [9, 14]. Although the EV concentration had increased 10fold, their ADAM10 content, and hence secretion of ADAM10 from melanoma cells, was reduced and correlated inversely with the increasing ratio of co-cultured Huh7 cells (Fig. 1f, lane 3, 4). Without co-culture, ADAM10 was strongly present in EV from MCTC (Fig. 1f, lane 2).

To confirm this suppressive effect, we analyzed the content of cytokines, chemokines and soluble factors (CCF) in EV (see list of analyzed factors in Supplementary Table 1) from MCTC before and after co-culture by protein microarray. While EV derived from MCTC contained a rich CCF profile, this profile was suppressed when MCTC were co-cultured with Huh7 cells in a cell ratio-dependent manner (Fig. 1g, gray boxes, red numbers; primary data in Supplementary Fig. 1b). On the other hand new factors were secreted upon co-culture (green numbers). These additional factors (yellow boxes), which included IFNγ, could have been secreted by both cell lines. Clearly, however, these factors were produced as a consequence of the interaction of both cell types.

We had previously demonstrated that pEV-associated miRNAs suppressed tumor cells [9] and suspected a similar mechanism in this co-cultures. Indeed, similar as in our recent study, we found an increase of MDM2/4 regulating and tumor cell suppressing miR-34a, miR-192 and miR-194 in EV of co-cultures (Fig. 1h). Conversely, EV derived from monocultures contained low concentrations of those miRNAs. Another MDM2/4 regulating miRNA, miR-215, was not significantly elevated. While we could not determine the cellular origin of those miRNAs, it seemed likely that they were produced by the Huh7 hepatocytes, due to their tumor-suppressive properties. Taken together, hepatocytes exerted a suppressive effect on MCTC, potentially executed by EV and associated factors, including miRNAs.

4.3. Hepatocyte/ tumor cell co-cultures secrete miRNAs also found in tumor patients

To substantiate the assumption of tumor-suppressive pEV derived from liver cells, we wanted to expand our analysis on EV from co-cultures. We speculated that co-cultures would [1] produce unique EV-associated factor profiles that might be detected in patients pEV and [2], that these factor patterns could hint at the potential cellular origin if a similar interaction occurred in vivo. For internal validation we decided to analyze two different factor sets, namely miRNAs and CCF.

We assessed EV miRNAs and CCF profiles from co-cultures (for 48 h) of 3 different liver cell types (as in Fig. 1b) with 3 different primary melanoma lines, each in two different co-culture ratios (1:1, 2:1). The same analysis was performed using resting PBMC from two different donors at a higher ratio of 30:1, since some PBMC sub-fractions, e.g. dendritic cells, are low in number. The results were compared with factors found in pEV from 12 melanoma patients and 2 healthy controls. Melanoma patients were randomly selected from three clinical stage groups, namely *Re*- (patients with a relapsing tumor), HR- (patients with a high risk for tumor relapse) and LR-patients (patients with a low risk for tumor relapse)) (Supplementary Table 2). In *Re*-patients, a tumor relapse was detected upon routine clinical presentation (every 3 month), irrespectively of the original clinical stage. A summary of this analysis scheme is presented in Fig. 2a. The pEV of these patients were purified by differential

centrifugation as described previously [9], their particle concentration was determined (Supplementary Fig. 2a) and divided into two aliquots. One aliquots was used to extract micro-RNAs, while the other aliquot was used to determine the CCF protein content by protein array (RayBiotec®; see below Supplementary Fig. 6a).

For the miRNA analysis the NanoString technology was used, performed by a qualified operator (service facility). From these data sets, obtained from 14 individuals and 32 mono- and co-cultures, only miRNAs were included showing at least a twofold increase over their respective reference categories (as defined in Supplementary Table 3). This procedure lead to a representative miRNA population for each patient and cell culture group as indicated by the Venn diagrams in Fig. 2b (list of miRNAs in Supplementary Table 4).

Analyzing the overlap between patient`s pEV and culture EV, we found that EV miRNAs from liver-melanoma co-cultures were significantly more present in pEV obtained from melanoma patients (in% of total) as compared to miRNAs from PBMC-melanoma co-cultures, or liver and PBMC monocultures (Fig. 2c, green box, chi-squared test). Importantly, these miRNAs were not found in healthy individuals. For example, all liver co-cultures produced a total of 67 miRNAs (Fig. 2c), which were at least 2-fold higher than in reference categories. Of those, 24 (37%) were found in patient`s pEV, namely 3 in *Re*-, 7 in HR- and 15 in LR patients (Fig. 2c, red box). Thus, LR- and HR patients, who suppress tumor relapse, harbored considerably more of liver co-culture-derived miRNAs as compared to *Re*-patients, who had lost control over tumor growth. MiRNA from all other cultures were not found in higher numbers. These results supported the assumption that an interaction between liver cells and tumor cells occurred in tumor patients and induced the secretion of liver-derived pEV.

4.4. Tumor cell suppression in liver-cell and PBMC co-cultures

Next we analyzed the CCF content of EV purified from the same in vitro cultures described in Fig. 2a. While EV secreted from liver cell mono-cultures contained very few factors, EV from all three melanoma cell lines, and the above described MCTC line, contained a prominent and overall similar CCF profile. Notably, ICAM1, MIF and MCP-1 were secreted by all 4 lines (Supplementary Fig. 2b).

Upon co-culture with liver cells these EV profiles changed significantly. Many of the factors secreted by tumor lines were strongly suppressed in a liver cell-ratio dependent manner (Fig. 3a, red boxes), as exemplified in for Huh7 hepatocytes (results for all liver lines in Supplementary Fig. 3, quantification in Supplementary Fig. 4). Conversely, some factors, which were not detected in either monoculture, were upregulated in a cell ratio-dependent manner (Fig. 3a, blue boxes). Analyzing the effects of all liver lines, each cell line showed an individual pattern of suppression and secretion (Fig. 3b) and each pattern was similar against the different tumor lines. Together these data suggested that liver cells reacted actively to the encounter of tumor cells.

A similar observation was made with PBMC. Resting PBMC did not secrete EV with a notable CCF content (Fig. 4a, upper graphs). Again, this changed significantly when tumor cells were co-cultured. Some of the tumor-derived factors were completely suppressed (Fig. 4a, lower graphs, red boxes), while other factors not present in PBMC or tumor cell monocultures were strongly upregulated (blue graphs). Both PBMC donors reacted similarly to all co-cultured melanoma tumor lines (Fig. 4b). Conversely, a co-culture of PBMC with Huh7 cells and primary fibroblasts had only a mild stimulating effect on few CCF factors (Supplementary Fig. 5). The strong PBMC reaction, was in part due to the HLA mismatch of the interacting tumor cells, which represents an immune response to multiple strong and weak foreign antigens, whereas an anti-tumor immune response reacts to normal host antigens overexpressed and/or mutated on tumor cells. Hence, the here measured pEV secretion may not occur at this strength in vivo.

4.5. EV/pEV factor comparison suggests tumor- and host-derived EV factors

The presence of EV CCF factors in the various in vitro cultures was summarized and compared with the relative presence of factors (CCF) detected in patient`s pEV. For this, patient's pEV had been analyzed by protein array (primary data in Supplementary Fig. 6a, quantified data in Fig. 5 below), similar as described previously [9]. To verify that these factors were secreted in vesicles, and were not attached as soluble factors to their surface, plasma samples from three different patients (LR, HR, *Re*) were purified by sucrose gradient and analyzed using a bead-antibody coupled system (Luminex®), detecting 6 different CCF factors. In pEV lysates, cytokines were detected similar as by protein array. Conversely, when pEV were not lysed, these positive reads were mostly negative. This implicated that the identified factors were contained within the pEV.

The average level of all detectable CCF factor in each patient group was color coded (Fig. 5a left rows). Deducing from this synopsis, factors were deemed "tumor-associated" when they were [1] present in *Re*- and absent in LR patients, [2] were produced by tumor cells and not by liver or PBMC monocultures, and [3] when they were absent and/or suppressed in liver and/or PBMC co-cultures. For example, MMP9 was strongly present in 4/4 *Re*-patients, but almost absent in HR (1/4) and LR patients (0/4). MMP9 was not produced by the liver or PBMC monocultures, but produced by all tumor lines. MMP9 was not present in liver or PBMC co-cultures, as it`s secretion from tumor cells was likely suppressed. Conversely, factors were deemed "liver/PBMC-associated", when they were [1] not detected in tumor cell monocultures, but [2] were present and [3] not suppressed in liver/PBMC co-cultures. For example, IFNγ was not produced in tumor monocultures, but strongly present and not suppressed in the liver/PBMC - tumor co-cultures. Hence, IFNγ likely derived from liver cells and/or PBMC. Using this algorithm, we assumed/assigned 6 of 24 factors to derive from tumor cell activity and 5 factors to derive from PBMC and/or liver cell activity (Fig. 5a, right column).

4.6. Tumor- or host-derived pEV factors correlate with clinical stage

To validate the assignment of these factors, we asked whether their relative presence correlated with the clinical stage (Fig. 5b and c). First we noticed that the presence, respectively absence, of two of the assigned markers (MMP9 and IFNγ) correlated with tumor relapse while their inverse presence/absence in HR and LR-patients correlated with tumor control. The same was true for two non-assigned factors, TIMP-1 and MCP-1 (Fig. 5b, red boxes).

We then counted all positive signals (>0.3 relative intensity in Fig. 5b) in each patient group (Fig. 5c, blue bars, white numbers), as well as the number of tumor- and liver/PBMC-associated signals (Fig. 5c red and green bars). First, all *Re*-patients harbored significantly more factors in their pEV (49) than HR (37) and LR-patients [22]. Second, in *Re*-patients a surprisingly high number of these signals represented tumor-assigned factors (21/49: 45%), but only a low number were liver/PBMC-associated (9/45:18%). In HR patients the ratio of tumor- and liver/PBMC-associated factors was evenly distributed (32% vs 34% respectively), whereas this ratio was inverted in LR patients (9% vs. 32%). In summary, our assignment of factors correlated surprisingly well with the clinical stage and risk for tumor relapse, showing more tumor and less liver/PBMC-associated factors in late stages, while the opposite was true in early stages.

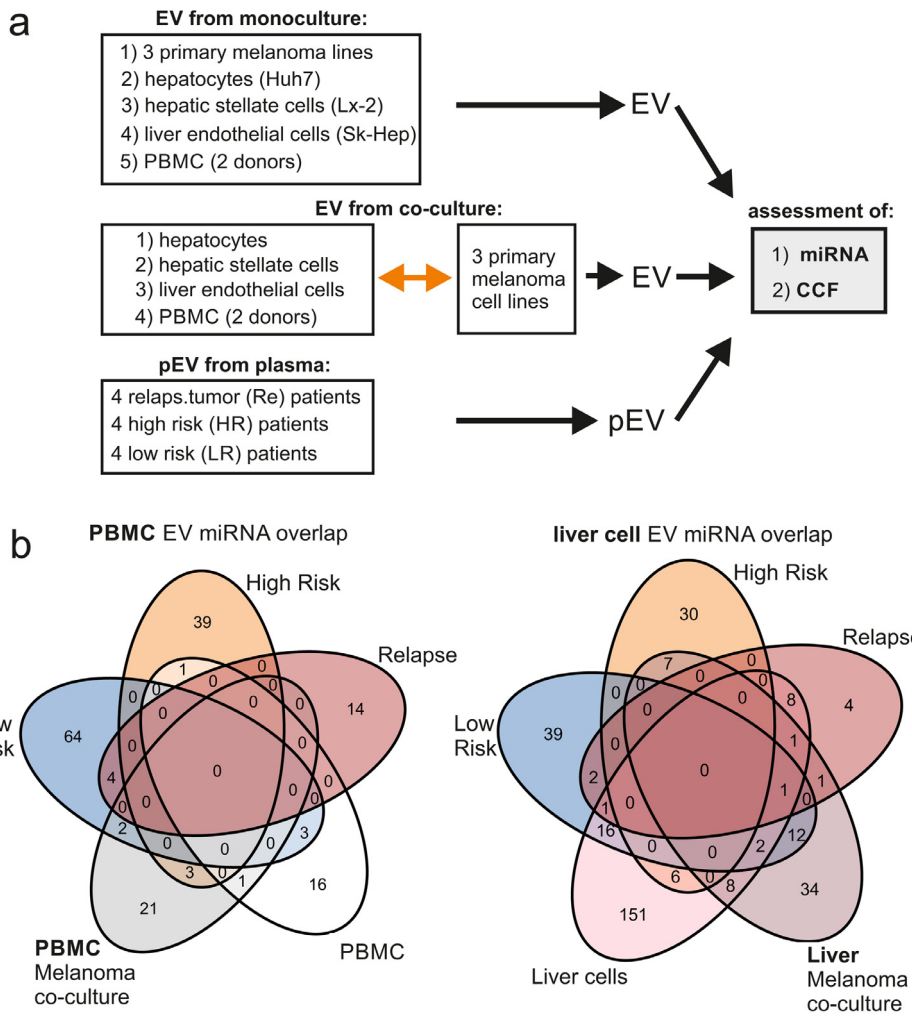

c

	miRNAs from culture		culture miRNAs found in: controls	melanoma patients				
	total miRNA	in Pat. pEV	Healthy	Relapse	High Risk	Low Risk	% of total	
liver monoclt.	197	36	1	11	6	20	18	p= 0.004
liver co-clt.	67	24	0	3	7	15	37	
PBMC monoclt.	21	4	0	0	1	3	19	
PBMC co-clt.	27	5	0	0	3	2	19	

Fig. 2. EV-associated miRNAs from co-cultures are found in melanoma patients. a Schematic overview of the experimental procedure described in the text. EV were purified by differential centrifugation either from cell monocultures or co-cultures as indicated. Similarly pEV were purified from 12 melanoma patients in the 3 different clinical stages (see text for details). Micro-RNAs and protein content were extracted from the vesicles and analyzed by commercially available test systems (NanoString, protein arrays). b Venn diagrams depicting the presence of upregulated miRNAs in each patient group and cell culture, and their respective overlap. An up-regulation was defined as at least a two-fold increase over reference- or category groups as explained in Supplementary Table 3. The overlap of miRNAs between selected categories was inspected using Venn diagrams. c Summary of the Venn diagrams depicted in (b). Imbalances in the miRNA distribution were checked on overlap-derived contingency tables with the chi-squared test. This revealed that miRNAs found in liver co-cultures (a total of 67) are also found in pEV of melanoma patients, particularly HR and LR patients (red box). Compared to the presence of miRNAs from liver monocultures (a total of 197), this was significant (green box; chi-squared test).

5. Discussion

We have recently demonstrated that post-operation tumor patients harbor elevated levels of tumor cell suppressive pEV. Based on indirect evidence, we now speculate that liver cells, beside PBMC, are a potential source of these cancer-induced pEV. Surprisingly, we also found evidence for a strong presence of tumor-derived pEV, implying that residual melanoma cells are potentially more numerous and more active than anticipated. Finally, we present preliminary results from patient material, indicating that patterns of pEV-derived factors could eventually serve to monitor cancer relapse.

At present no technology exists that could reliably trace pEV to their cellular origin, since none of the proteins and factors contained therein are truly unique for a specific organ or tissue. Hence, our assignment of factors to tumor- or liver/PBMC cell origin on the basis of their respective absence/presence in pEV and EV from in vitro cultures (Fig. 5a) remains an assumption. Nevertheless, there are several arguments that support our approach and conclusion/hypothesis. First, liver cells and PBMC reacted strongly upon encounter of tumor cells as demonstrated here (e.g. Fig. 1e). It should be noted, that Kupffer and sinus endothelial cell are most likely the first cells to encounter tumor cells directly. On the other hand, host cells, including hepatocytes, may sense the activity of tumor cells through

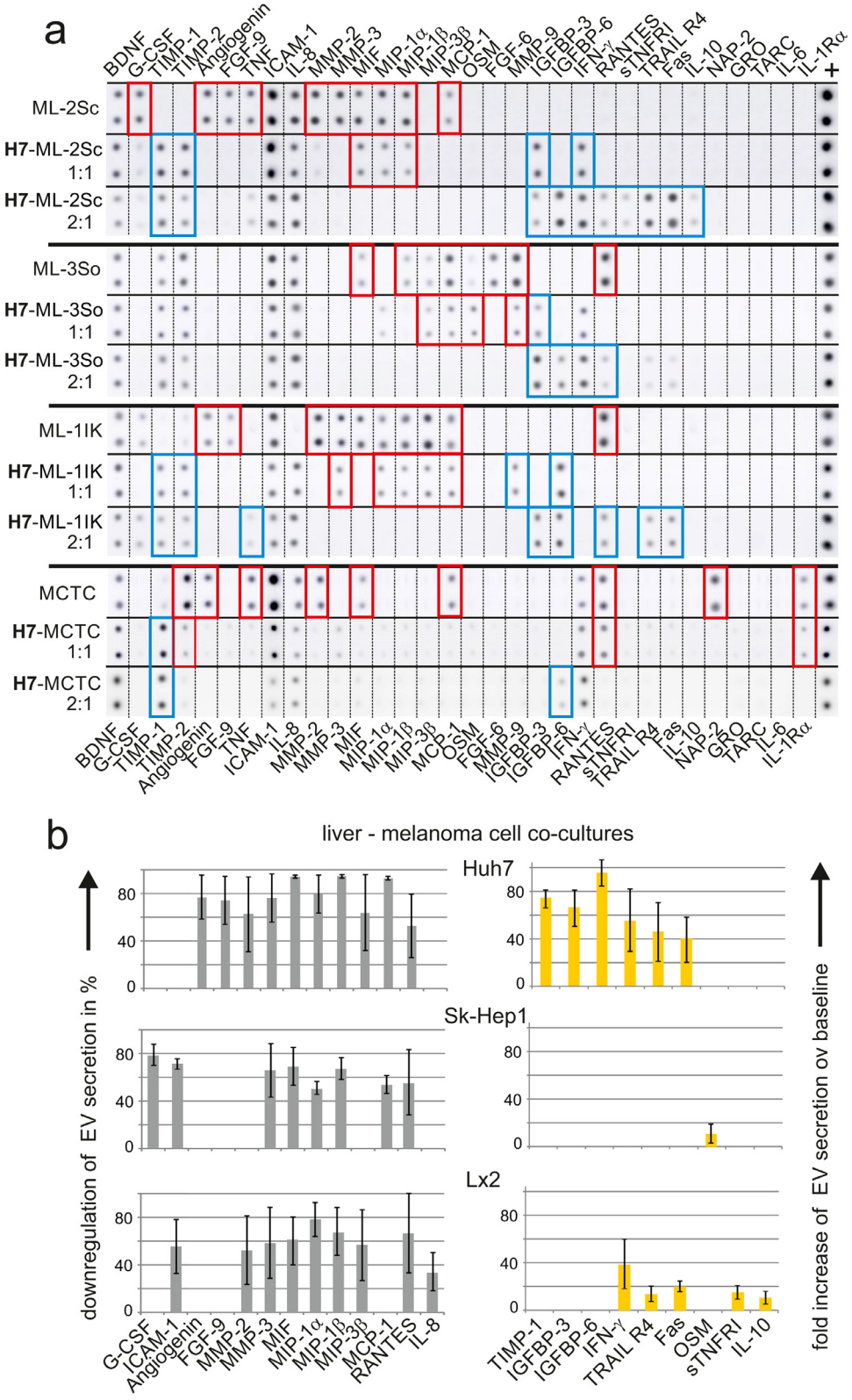

Fig. 3. CCF factors detected in EV of liver/melanoma co-cultures. a Protein arrays of EV from melanoma cells before and after co-culture with Huh7 hepatocytes. Shown are original signals serving as the basis to calculate the pixel density and relative concentration of CCF in the indicated liver cell mono-cultures and liver/melanoma co-cultures. The cells were cultured or co-cultured for 48 h at a ratio of 1:1 and 2:1, before being purified and analyzed. The original signals were rearranged for better overview and comparison. Down-regulated melanoma-derived factors are indicated by red boxes, whereas up-regulated factors are indicated by blue boxes. b Summary of EV CCF regulation in liver/melanoma co-cultures. Based on the data/numbers shown in (a), mean values and error bars [student *t*-test] were calculated for the effect of each liver line on all 3 melanoma lines (MCTC not included). Only factors are shown and analyzed that were up or down regulated in any of the co-cultures. The gray bar diagrams depict the relative down regulation of EV secretion with respect to the levels seen in melanoma mono-cultures. The yellow bars depict the relative up-regulation of new CCF factors, expressed as fold increase over baseline levels in melanoma, liver and PBMC mono-cultures.

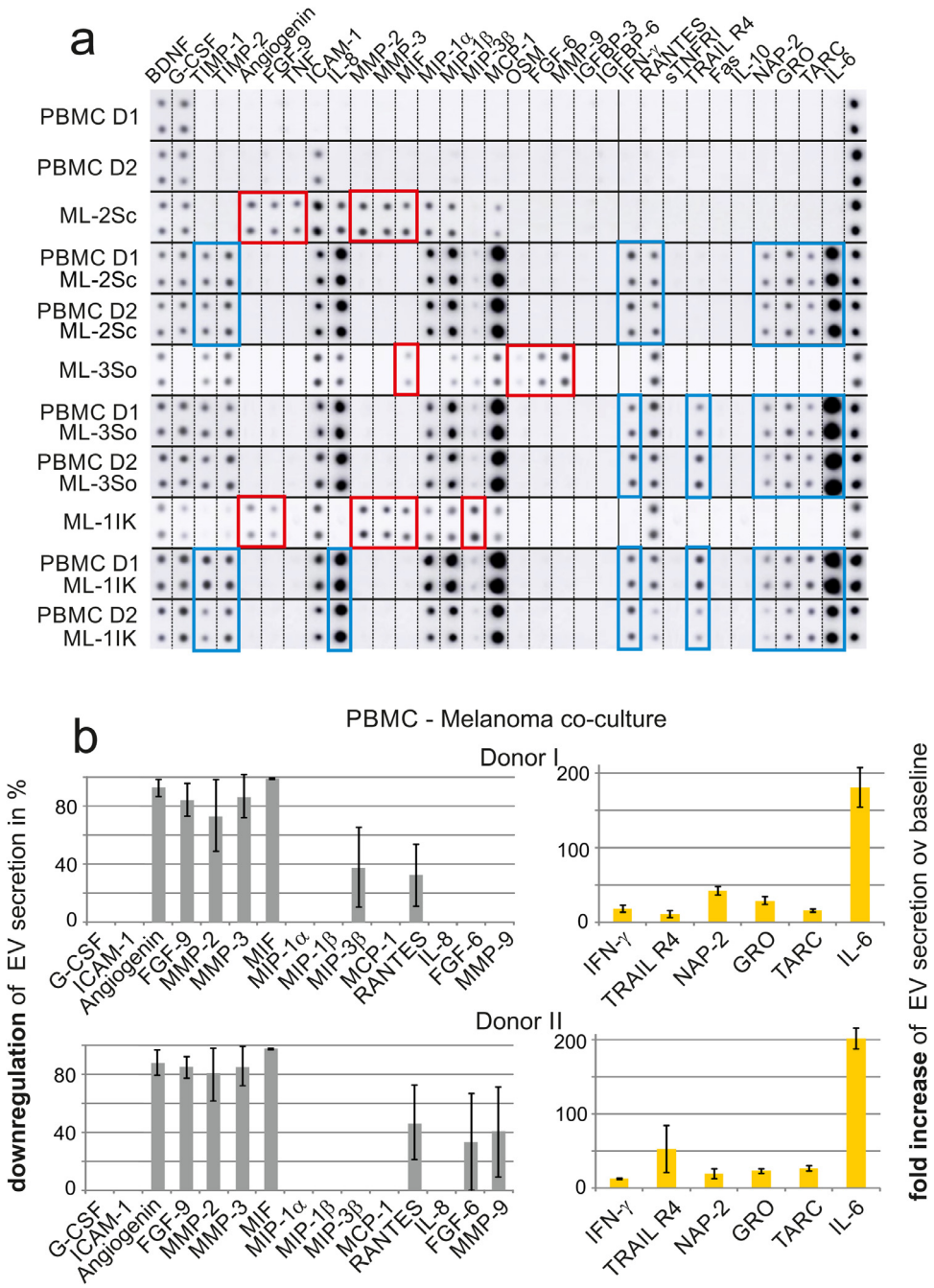

Fig. 4. CCF factors detected in EV from PBMC/melanoma co-cultures. a Protein arrays of EV from melanoma cells before and after co-culture with PBMC. Shown are rearranged original signals as in Fig. 3a of CCF protein arrays with purified EV from PBMC mono- and PBMC/melanoma co-cultures. Only resting PBMC were used. The cells were cultured or co-cultured for 48 h at a ratio of 30:1, before being processed as in Fig. 3a. Down-regulated melanoma-derived factors are indicated by red boxes, whereas up-regulated factors are indicated by blue boxes. b Summary of EV CCF regulation in PBMC/melanoma co-cultures. Based on the data/numbers shown in (a), mean values and error bars [student *t*-test] were calculated for each factor secreted by both PBMC donors upon co-culture with all 3 melanoma lines similar as in Fig. 3b.

secreted factors, e.g. cytokines and tumor vesicles, and potentially through their secretion of RNA elements and endogenous retroviruse [20, 21]. Taken together, even when we take the HLA mismatch in our in vitro system into account, a reduced, but similar reaction is likely to occur in vivo. Nevertheless, this HLA mismatch is certainly a limitation of this in vitro system, and the innate PBMC reaction/pEV secretion could be minimal, or even absent in many instances. However, this would not affect our conclusions with respect to the assignments of the pEV factors in Fig. 5a. Second, we analyzed patterns of factors and micro-RNAs, and not single markers (Fig. 5b). Third, the presence/absence of tumor- and liver/PBMC-associated pEV factor patterns, including miRNAs, correlated surprisingly well with the clinical stage and tumor relapse (Fig. 2c, 5b and c). Finally, this reaction did not kill tumor cells, as would have been expected for an innate immune interaction, e.g. by NK cells, but resulted in a seemingly tumor cell-suppressive activity, including the upregulation of p53/β-catenin suppressive miRNAs [9] (Fig. 1f–h). Cell killing by circulating pEV, as demonstrated previously by DC-derived EV [9], would likely cause more harm than protection.

Growing tumors may shed large amounts of cells into circulation [22]. Not all of these cells will be readily recognized and killed by the adaptive immune system. Hence innate immune cells are likely the

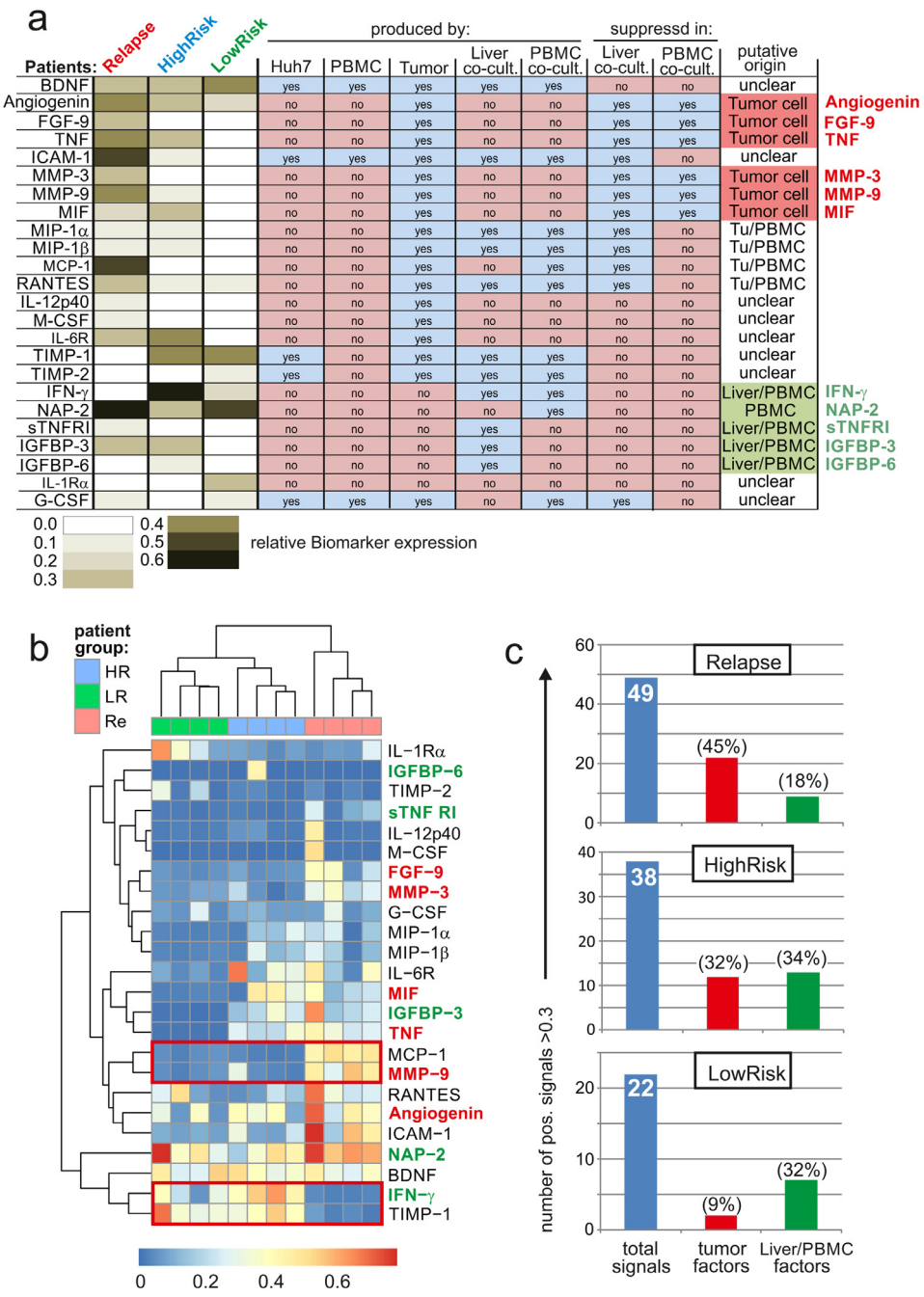

Fig. 5. Tumor- and liver/PBMC-derived factors correlate with the clinical stage. a pEV factors in melanoma patients and their presence/absence in cell culture derived EV. Depicted on the left are factors found in patient's pEV. Their relative/average levels were calculated on the basis of protein array signals (Supplementary Fig. 6a) using ImageJ. Values were normalized with respect to the internal positive controls and different levels of expression were color coded for each patient group. The presence/absence (yes/no) of these factors in all cultures and co-cultures was determined accordingly, based on results in Fig. 3 and 4. Based on this information their putative cellular origin was deduced (right row), in an algorithm explained in the text. b CCF factor abundance in melanoma pEV correlates with the clinical stage. The CCF factors quantified in patient's pEV were depicted by heat map. Factors depicted in red letters are of putative tumor cell origin and factors in green letters of putative liver/PBMC origin as predicted by the algorithm in (a). Red boxes are explained in the text. c Abundance of tumor- and liver/PBMC-assigned pEV factors correlates with clinical stage. The blue bars depict the number of all positive CCF signals found in each melanoma patient group (4 patients in each group). The red and green bars depicts the number of tumor-associated factors (red) and liver/PBMC associated factors (green) in each patient group as determined in (a). The respective percentages were calculated with respect to the total number of signals and depicted in parenthesis.

first line of defense against a growing and immunologically changing tumor [23]. It is at least plausible that the liver plays an important role in this scenario as it is a large immune sensing organ screening the whole blood volume every 3 min [24]. In addition, it has the size and secretory capacity to supply pEV in high numbers. Liver cells may sense circulating tumor cells through direct contact, as demonstrated here in vitro, or by secreted factors, e.g. cytokines and tumor vesicles, and potentially through tumor cell typical secretion of RNA elements and endogenous retroviruses [20, 21]. Hence, remaining tumor cells after R0 surgery (CTC/DTC) may stimulate liver cells and PBMC for low, but persistently elevated pEV levels.

The strong presence of markers, particularly in relapsing (*Re*) patients (Fig. 5a), that we speculated to be secreted from tumor cells, was surprising, because the number of CTC/DTC is generally considered to be very low [25]. It is assumed that most CTC/DTC die rapidly, as shown in animal models [26, 27]. However, the situation in HR-

and particularly in relapsing patients may be somewhat different from experimental systems. CTC/DTC cell clones may have learned to proliferate while escaping immune surveillance. In addition, the growing tumor mass in *Re*-patients likely contributes significantly to the presence of tumor cell-derived pEV. In any scenario, such pEV secreting tumor cells, and potentially also their tumor microenvironment [28, 29], would have to proliferate to significant numbers in order to produce the amount of pEV-associated factors measured in this study in plasma.

The pattern of tumor and immune-derived factors secreted by pEV, if correct, could provide a snapshot-like insights into the battle between the immune system and tumor cells. Our preliminary analysis of these patterns in three different clinical stages of melanoma supported this assumption and revealed an astonishing discriminatory power of these patterns (Fig. 5b). This was particularly apparent between high-risk patients that controlled their CTC/DTC tumor compartments and those patients experiencing a tumor relapse. The presence/absence of four factors (MCP-1, MMP-9, IFNγ and TIMP-1) correlated well with tumor control and tumor relapse. With the help of artificial intelligence and higher case numbers, more information could potentially be extracted from these patterns than demonstrated here. Hence, such pEV factor patterns could eventually become diagnostics tools in the management of cancer patients.

In summary our results imply that tumor cells are sensed by the innate immune system, including liver cells, inducing a pEV-mediated reaction aimed to silence but not kill tumor cells. Notably, our results also imply that CTC/DTC are more prevalent and/or more active than currently believed, otherwise we might not see the rich CCF and miRNA response in patient`s pEV. Finally, the profile of pEV-associated factors may help to estimate the relative risk for melanoma relapse. However this requires the analysis of large numbers of patient plasma samples.

Contributors

The project was designed and coordinated by A.S.B. Substantial contributions to the work were made by J-H.L. (pEV purification, cell transfections, Western blots, protein arrays and pEV analysis); M.E. and J. V. (Bioinformatics); K.B. (pEV purification, miRNA purification). All authors read and approved the final version of the manuscript.

Funding

German Federal Ministry of Education and Research (BMBF) (01GU1107A) and e:Bio MelEVIR (031L0073A) and by the IZKF Erlangen (*Interdisziplinäres Zentrum für Klinische Forschung*). J.V. acknowledges support by the BMBF e:Bio miRSys (0316175A) and e:Bio MelEVIR (031L0073A). J.V. also acknowledges support from the Elan Funds of the Medical Faculty of the Friedrich-Alexander University of Erlangen-Nürnberg (FAU) and the DFG through the project SPP 1757/1 (VE 642/1−1).

Data sharing statement

The miRNA data sets are available at NCBI's Gene Expression Omnibus under the ID GSE100508.

Declaration of Competing Interest

Dr. Eberhardt reports grants from German Ministry of Education and Research, during the conduct of the study. The other authors declare that there is no actual or potential conflict of interest in relation to this article. They have no relationships relevant to the contents of this paper to disclose.

Acknowledgements

This work was supported by the German Federal Ministry of Education and Research (BMBF) (01GU1107A) and MelEVIR (031L0073A) (JH.L.) and by the IZKF Erlangen (Interdisziplinäre Zentrum für Klinische Forschung). J.V. and M.E. were supported by the BMBF as part of the projects eBio:miRSys (0316175A) and eBio:MelEVIR (031L0073A). J.V-G. is also funded by the Elan Funds of the Medical Faculty of the Friedrich-Alexander-University of Erlangen-Nürnberg (FAU) and the DFG through the project SPP 1757/1 (VE 642/1−1).

Supplementary materials

Supplementary material associated with this article can be found in the online version at doi:10.1016/j.ebiom.2020.103119.

References

[1] Nolan JP, Jones JC. Detection of platelet vesicles by flow cytometry. Platelets 2017;28(3):256–62.
[2] Zaldivia MTK, McFadyen JD, Lim B, Wang X, Peter K. Platelet-derived microvesicles in cardiovascular diseases. Front Cardiovasc Med 2017;4:74.
[3] Melo SA, Luecke LB, Kahlert C, Fernandez AF, Gammon ST, Kaye J, et al. Glypican-1 identifies cancer exosomes and detects early pancreatic cancer. Nature 2015;523(7559):177–82.
[4] Yang KS, Im H, Hong S, Pergolini I, Del Castillo AF, Wang R, et al. Multiparametric plasma EV profiling facilitates diagnosis of pancreatic malignancy. Sci Transl Med 2017;9(391).
[5] Barros FM, Carneiro F, Machado JC, Melo SA. Exosomes and immune response in cancer: friends or foes? Front Immunol 2018;9:730.
[6] Gao L, Wang L, Dai T, Jin K, Zhang Z, Wang S, et al. Tumor-derived exosomes antagonize innate antiviral immunity. Nat Immunol 2018;19(3):233–45.
[7] Coppe JP, Desprez PY, Krtolica A, Campisi J. The senescence-associated secretory phenotype: the dark side of tumor suppression. Annu Rev Pathol 2010;5:99–118.
[8] Terlecki-Zaniewicz L, Lammermann I, Latreille J, Bobbili MR, Pils V, Schosserer M, et al. Small extracellular vesicles and their miRNA cargo are anti-apoptotic members of the senescence-associated secretory phenotype. Aging (Albany NY) 2018.
[9] Lee JH, Dindorf J, Eberhardt M, Lai X, Ostalecki C, Koliha N, et al. Innate extracellular vesicles from melanoma patients suppress beta-catenin in tumor cells by miRNA-34a. Life Sci Alliance 2019;2(2).
[10] Lee JH, Schierer S, Blume K, Dindorf J, Wittki S, Xiang W, et al. HIV-Nef and ADAM17-containing plasma extracellular vesicles induce and correlate with immune pathogenesis in chronic HIV infection. EBioMedicine 2016;6:103–13.
[11] Flaumenhaft R. Formation and fate of platelet microparticles. Blood Cells Mol Dis 2006;36(2):182–7.
[12] Rand ML, Wang H, Bang KW, Packham MA, Freedman J. Rapid clearance of procoagulant platelet-derived microparticles from the circulation of rabbits. J Thromb Haemost 2006;4(7):1621–3.
[13] Klein CA. The biology and analysis of single disseminated tumour cells. Trends Cell Biol 2000;10(11):489–93.
[14] Lee JH, Wittki S, Brau T, Dreyer FS, Kratzel K, Dindorf J, et al. HIV Nef, paxillin, and Pak1/2 regulate activation and secretion of TACE/ADAM10 proteases. Mol Cell 2013;49(4):668–79.
[15] Boland GM, Gershenwald JE. Principles of melanoma staging. Cancer Treat Res 2016;167:131–48.
[16] Irizarry RA, Warren D, Spencer F, Kim IF, Biswal S, Frank BC, et al. Multiple-laboratory comparison of microarray platforms. Nat Methods 2005;2(5):345–50.
[17] Benjamini Y, Drai D, Elmer G, Kafkafi N, Golani I. Controlling the false discovery rate in behavior genetics research. Behav Brain Res 2001;125(1−2):279–84.
[18] Tusher VG, Tibshirani R, Chu G. Significance analysis of microarrays applied to the ionizing radiation response. Proc Natl Acad Sci U S A 2001;98(9):5116–21.
[19] Lee JH, Ostalecki C, Zhao Z, Kesti T, Bruns H, Simon B, et al. HIV activates the Tyrosine Kinase Hck to Secrete ADAM Protease-Containing Extracellular Vesicles. EBioMedicine 2018.
[20] Kassiotis G, Stoye JP. Immune responses to endogenous retroelements: taking the bad with the good. Nat Rev Immunol 2016;16(4):207–19.
[21] Balaj L, Lessard R, Dai L, Cho YJ, Pomeroy SL, Breakefield XO, et al. Tumour microvesicles contain retrotransposon elements and amplified oncogene sequences. Nat Commun 2011;2:180.
[22] Massague J, Obenauf AC. Metastatic colonization by circulating tumour cells. Nature 2016;529(7586):298–306.

[23] Woo SR, Corrales L, Gajewski TF. Innate immune recognition of cancer. Annu Rev Immunol 2015;33:445–74.
[24] Jenne CN, Kubes P. Immune surveillance by the liver. Nat Immunol 2013;14(10):996–1006.
[25] Nagrath S, Sequist LV, Maheswaran S, Bell DW, Irimia D, Ulkus L, et al. Isolation of rare circulating tumour cells in cancer patients by microchip technology. Nature 2007;450(7173):1235–9.
[26] Wong CW, Lee A, Shientag L, Yu J, Dong Y, Kao G, et al. Apoptosis: an early event in metastatic inefficiency. Cancer Res 2001;61(1):333–8.
[27] Heyn C, Ronald JA, Ramadan SS, Snir JA, Barry AM, MacKenzie LT, et al. In vivo MRI of cancer cell fate at the single-cell level in a mouse model of breast cancer metastasis to the brain. Magn Reson Med 2006;56(5):1001–10.
[28] Straussman R, Morikawa T, Shee K, Barzily-Rokni M, Qian ZR, Du J, et al. Tumour micro-environment elicits innate resistance to RAF inhibitors through HGF secretion. Nature 2012;487(7408):500–4.
[29] Smith MP, Sanchez-Laorden B, O'Brien K, Brunton H, Ferguson J, Young H, et al. The immune microenvironment confers resistance to MAPK pathway inhibitors through macrophage-derived TNFalpha. Cancer Discov 2014;4(10):1214–29.